



Assessing the large-scale plant-water relations using remote sensing products in the humid subtropical Pearl River Basin in south China

Hailong Wang^{1,2,3}, Kai Duan^{1,2,3}, Bingjun Liu^{1,2,3}, Xiaohong Chen^{1,2,3}

¹ School of Civil Engineering, Sun Yat-sen University, Guangzhou, Guangdong, China, 510275

5 ² Guangdong Engineering Technology Research Center of Water Security Regulation and Control for Southern China, Sun Yat-sen University, Guangzhou, China, 510275

³ Southern Marine Science and Engineering Guangdong Laboratory, Zhuhai, Guangdong, China, 519082

Correspondence to: Hailong Wang (wanghlong3@mail.sysu.edu.cn; whl84@hotmail.com)

Abstract. Vegetation interact closely with water resources. Conventional studies of plant-water relations at the field scale
10 are fundamental for understanding the mechanisms of how plants alter and adapt to environmental changes, while large-scale
studies can be more practical for regional land use and water management towards mitigating climate change impacts. In this
study, we investigated the changes in total water storage (TWS), aridity index (AI) and vegetation greenness, productivity
and their interactions in the Pearl River Basin since 2002. Results show overall increase of TWS especially in the middle
15 reaches where vegetation greenness and productivity also increased. This region dominated by croplands was identified as
the hotspot for changes and interactions between water and vegetation in the basin. Vegetation was more strongly affected
by TWS than precipitation (P) at both the annual and monthly scales. Further examination showed that the influence of P on
vegetation in wet years was stronger than dry years, while the TWS impact was stronger in dry years than wet years;
moreover, greenness responded faster and productivity slower to dryness changes in dry years than wet years. The lag effects
20 resulted in nonlinearity between water and vegetation. This study implies that vegetation in the basin uses rainwater prior to
water storage until it gets dry, and the degree of water restriction on vegetation was higher than that of water consumption by
vegetation even in this rain-abundant region.

1 Introduction

Vegetation covers 70% of the land surface, playing a vital role in water, carbon and energy exchanges between land and
atmosphere (Yang et al., 2016). As climate change has been more and more evident since the industrial age (Marvel et al.,
25 2019; Sippel et al., 2020) which results in numerous ecohydrological problems such as droughts, flooding, tree mortality,
etc., managing land use especially vegetation cover has been considerably practiced in many catchment planning projects
(Adhami et al., 2019; Stewardson et al., 2017). The theoretical basis is that vegetation can intercept precipitation by the
canopy which helps with flood control (Soulsby et al., 2017; Wheater and Evans, 2009); uptake soil water or groundwater
and transpire it through leaves to increase moisture in the air; create macropores for water flow paths in soils to aid rapid
30 recharge to soil water stores (Ghestem et al., 2011). In addition, vegetation assimilates carbon dioxide (CO₂) through



photosynthesis to accumulate biomass production and reduce greenhouse gas concentration (Notaro et al., 2007; Yosef et al., 2018). In turn, atmospheric and hydrologic conditions can affect vegetation health by altering vegetation physiological characteristics (Reyer et al., 2013; Sala et al., 2010). Therefore, investigation of plant-water relations is of great importance in maintaining terrestrial hydrological regimes and mediating carbon cycle and energy balance in the Earth systems.

35 Conventional studies of plant-water relations are often carried out at the leaf and canopy level based on extensive field measurements. There are rich literatures that examine the plant responses such as stomatal opening/closure to stress induced by both atmospheric condition and water supply (Martin-StPaul et al., 2017). For instance, plant water use responded sensitively to rainfall pulses in dry semi-arid areas (Huang and Zhang, 2015; Plaut et al., 2013), whilst the light exposure (i.e. energy) between frequent low-intensity rainfall events seemed more important to stimulate transpiration than rainfall itself in

40 some humid low-energy boreal regions (Wang et al., 2017). Soil water especially the root-zone moisture plays a key role in plant growth. The relationship is commonly characterized as linear increase of plant water use with increasing moisture within a certain range above which plant water use maintains its potential rate and will be limited mainly by energy (Novák et al., 2005). Noticeably, some studies observed a parabolic relationship between plant water use and soil moisture (Zhao and Liu, 2010) or groundwater level (Liu et al., 2014a).

45 The site-specific (in terms of species, soil and climate) studies are fundamental for deep understanding of the mechanisms of how plants alter and adapt to environmental changes (Massmann et al., 2018; Petr et al., 2015; Susmilch and McAdam, 2017). However, it is difficult to draw universal conclusions about plant-water relations extrapolative to a large landscape comprised of many vegetation types and with different structures from site-specific analysis (Aranda et al., 2012; Wang et al., 2008). This would weaken the applicability of research outcomes on vegetation related ecological projects such as the Grain

50 for Green and Three-North Shelterbelt Project in China to assess the long-term impacts and feedback between climate, vegetation and hydrology (Liang et al., 2015). Assessing and mitigating climate change impacts such as floods and droughts (Fowler et al., 2019; Ma et al., 2015) require integrated efforts at a catchment scale. From this perspective, it is necessary to investigate the plant-water relations at a larger scale beyond field sites.

Remote sensing (RS) products provide abundant information on land surface hydrology and vegetation characteristics and

55 can be beneficial in overlooking the plant-water relations from a large spatial area. Over the past several decades, various RS data have been applied in many fields such as water budget assessment and hydrological components estimation (Pham-Duc et al., 2019; Wang et al., 2014a), vegetation phenology and the climate change impacts (Güsewell et al., 2017; Hwang et al., 2018), ecosystem services and its linkages with climate and land use (Xiao et al., 2019), etc. The advantage of RS analysis is that it can identify the interplay between water and vegetation over a long period and under a wide spatial coverage, and it is

60 promising in assisting the land and water management by pinpointing the hotspots for these changes and interactions.

An interesting and meaningful argument exists in the studies of plant-water relations. On the one hand, vegetation need water to survive and thus are directly influenced by water availability; on the other hand, vegetation are effective conduits to return water to the atmosphere, and can cause big water security concerns if the water carrying capacity for vegetation is exceeded (Xia and Shao, 2008). The most severe ecological degradation being faced by many inland river basins is closely



65 related to water availability (Yu and Wang, 2012). Meanwhile, in most cases an increase in forest cover will reduce water
yield and soil water storage (Brown et al., 2005; Schwärzel et al., 2020) because of an increase in evapotranspiration, though
the magnitudes are subject to scale, species and catchment size (Blaschke et al., 2008; Wang et al., 2008). Numerous studies
prove that many ecosystems are sourcing soil water recharged by precipitation or groundwater, therefore, plant water use
varies largely with rainfall pulses or groundwater level in such ecosystems especially in the drylands (Eamus and Froend,
70 2006; Xu et al., 2016; Yang et al., 2014). It is worth mentioning that majority of such studies were carried out in semi-arid
regions because of the urgent need to find an equilibrium between ecological restoration and water resources in these water-
limited areas. However, in the humid or semi-humid areas with abundant rainfall, it is still unclear whether the restriction of
water on vegetation or the consumption of water by vegetation prevails in the long term.

Despite previous studies examining the changes in hydrologic compartments, climate change and vegetation, there are few
75 insightful studies quantifying how hydroclimate and vegetation greenness and productivity interact at different time scales
and under contrast dryness conditions in the subtropical Pearl River Basin in China over the recent 2 decades. Thus, this
study is the first attempt to reveal the plant-water relations at a large spatial scale in the basin. Specifically, the objectives
include (1) characterizing the spatiotemporal patterns of hydroclimate and vegetation change in the last 13 years or so, and
identifying the hotspots for the changes; (2) quantifying the plant-water relations at different temporal scales under different
80 dryness conditions; and (3) examining the interactive role of water availability and vegetation growth. Results of this study
can be informative for the basin-wide land and water use planning under a changing environment.

2 Data and Methods

2.1 Study area

The Pearl River (in the range of 102–116°E, 21–27°N) ranks the second largest in China in terms of streamflow with a
85 drainage area of ~450,000 km² (Fig. 1), supporting the socioeconomic development of one of the most prosperous bay areas
of China. The climate of the Pearl River Basin (PRB) is characterized as subtropical, mainly influenced by the eastern Asian
monsoon and typhoons. The long-term mean annual temperature across the basin is 14–22°C, and mean annual precipitation
is 1200–2200 mm (Chen et al., 2010), primarily falls as rain and concentrates in April–September. The elevation is as high as
~2900 m in the west upland and decreases dramatically to the delta in the southeast, creating a gradient of ~3000 m.

90 The dominant vegetation is forest of evergreen species (~65.3%), followed by cropland (~18.1%) distributed mainly in the
middle of the basin along a northeast-southwest transect, where happens to be in the transitional areas of high-to-low
elevations in Guangxi province. Grassland (~9.3%) is the third largest land cover type mostly located in the west upland.
Due to the downstream location, flat terrain, and rapid population growth and economic development, the Pearl River Delta
tends to be more and more vulnerable under natural hazards such as flood and storm surge in wet seasons and saltwater
95 intrusion in dry seasons (Liu et al., 2019). In the recent 2 decades, droughts were found to occur frequently in the basin and
affected water allocation to different municipal areas and industries (Deng et al., 2018; Xu et al., 2019).



2.2 Data sources, pre-processing and analysis

To assess the plant-water relations at a large spatial scale, we obtained hydroclimate and vegetation data from different sources. Precipitation (P) and potential evapotranspiration (ET_p) were obtained from Global Land Data Assimilation System (GLDAS) (Rodell et al., 2004); aridity index (AI) was then calculated as the ratio of ET_p to P to represent the dryness condition. Total water storage (TWS) change is inferred by the mass change detected by GRACE satellites (Tapley et al., 2004). GRACE data can be accessed from the Jet Propulsion Laboratory (JPL), the Center for Space Research (CSR), and the German Research Centre for Geosciences. Previous studies have shown that the ensemble mean of different products is effective in reducing the noise in the gravity field solutions (Long et al., 2017; Sakumura et al., 2014). Here we used total water storage anomaly (TWSA) data from the JPL and CSR with ‘mascons’ solution (release 6) at a resolution of 0.5° and monthly. Cubic spline interpolation was applied to estimate the missing monthly data for the GRACE_{JPL} and GRACE_{CSR} products during 04/2002–03/2015 that cover 13 hydrological years.

Vegetation data in this study include Normalized Difference Vegetation Index (NDVI) and Gross Primary Production (GPP). NDVI was obtained from the GIMMS project during 04/2002–03/2015 and resampled to 0.5° using the nearest neighbor method and averaged to monthly to match the spatiotemporal resolution of GRACE and GLDAS data. Monthly GPP was obtained from the Numerical Terradynamic Simulation Group in the University of Montana and rescaled to 0.5° (Running et al., 2004). Information of data sources, resolution and time span for all variables related to this study is listed in Table 1. To compare with GRACE data, anomalies of P, AI, NDVI, and GPP data were calculated by subtracting the means over the same baseline period of GRACE data (i.e. 01/2004–12/2009).

To investigate the changes in hydroclimate and vegetation, we carried out trend analysis using the Mann-Kendall (MK) test method both in space and in time. The MK test does not require normality of time series and is less sensitive to outliers and missing values (Pal and Al-Tabbaa, 2009). This non-parametric test method has been used in many studies to detect changing hydrological regimes (Déry and Wood, 2005; Zhang et al., 2009). Interplay between hydroclimate and vegetation was quantified by linear regression; the Pearson correlation coefficient (r) and coefficient of determination (R^2) were taken as a measure for assessment of the linkages between different variables. Furthermore, a lag effect analysis was carried out to determine the temporal dependency between variables where the linear relationship was not obvious.

Since the interactions between hydroclimate and vegetation can be different under dry and wet conditions, we hereby selected dry and wet years according to the anomalies of TWS, NDVI and AI under the criteria that dry conditions correspond to negative anomaly values of TWS and NDVI in addition to high anomaly of AI. Then the relationships between hydroclimate dynamics and vegetation greenness and productivity were specifically analysed. Uncertainties of the data used were estimated by the standard error of each variable at the monthly and annual scales.



3 Results

3.1 Changes in water storage and dryness

Comparison of the GRACE data from JPL and CSR shows that mean annual TWSA from GRACE_{JPL} was overall greater than that from GRACE_{CSR} (Fig. 2a-b). Both products showed clear zonal characteristics similar to the average of the two (Fig. 2c) that TWSA was generally higher in the middle-to-east areas than the rest of the basin especially the west upland, which infers a generally wetting condition in comparison to the baseline period. The trends of annual TWSA (Fig. 2d) showed that over the 13 hydrological years the TWS in most of the basin has increased at a rate below 10 mm yr⁻¹ with 46% in the range of 5.0–10.0 mm yr⁻¹. Areas with low changing rate were mainly located in the west upland where the predominant land cover is grassland. Like the distribution of TWSA, water storage increase rate was also higher in the middle-to-east areas, where overlap partly with croplands, than the rest of the basin.

Temporally, the basin has been getting wetter in general from 2002 (Fig. 2e). The TWSA has increased over the 13 years by 6.8 mm yr⁻¹ inferred by GRACE_{JPL} and 4.6 mm yr⁻¹ by GRACE_{CSR}, with an average of 5.9 mm yr⁻¹. Noticeably, there were three shifts in the drying and wetting tendencies over the study period, i.e. the shift from drying between 2002 and 2005 to wetting between 2005 and 2008, followed by the shift back to drying between 2008 and 2011, and finally the shift to wetting after 2011. In the following sections, only the mean TWSA from GRACE_{JPL} and GRACE_{CSR} was used for analysis.

Figure 3 shows the aridity index (AI) characterizing the spatial and temporal patterns of dryness. Majority of the basin has a semi-humid climate (AI=1.0~1.5); the west upland was clearly drier than the rest of the basin which is associated with precipitation patterns. Although dryness condition has not changed significantly over the 13 years with an overall positive trend in space (0.004±0.012) and time (0.007), it has some interesting characteristics such as the drying tendencies primarily located in the southern areas, and the alternate periodical wetting and drying episodes temporally like TWSA. Areas with low TWS change rates coincided with drying climate represented by aridity index.

3.2 Changes in vegetation greenness and productivity

Spatial NDVI distributions (Fig. 4) were highly related to vegetation cover types that the high NDVI values coincided with forest covers and low values corresponded to impervious surfaces, grasslands and croplands. It clearly reflects the impacts of urbanization on surface greenness particularly near the basin outlets in the southeast. Over the 13 years NDVI has not shown significant changes across the basin, since the majority (~70%) had a MK test $p > 0.05$ at the pixel scale. The areas with significant changes were concentrated in the central south of the basin where croplands are predominant. This infers an intensification of crop farming activities over these areas.

Temporally, NDVI has an overall insignificant increase trend over the 13 years at an annual rate of 0.004 ($p=0.56$) with interannual fluctuations. It is noticeable that the periodical shifts in the NDVI trends were almost identical to TWSA in Fig. 2e. This reflects a tight bound between the vegetation greenness and water availability in this rain-abundant region. Interestingly, in 2004 when water storage continued to decrease following the previous years, NDVI did not show a



continuity of decreasing but increased instead, implying a vegetation resilience and recovery after previous dry period. The
160 recovery coincided with a slight decrease in aridity index, hence, vegetation did not respond solely to water availability but
also to atmospheric demand.

In addition to NDVI, GPP was also analysed for the basin (Fig. 5). It is not surprising to observe that GPP was highly
responsive to NDVI such that areas with low NDVI also had low GPP (e.g., the central agricultural region and upland
grassland). GPP anomaly also showed positive high values in the central south areas dominated by croplands coincident with
165 NDVI anomaly, indicating an increased agricultural production induced by intensified agricultural activities in this region. It
should be noted that most of the trends were not statistically significant. Over the entire basin, annual GPP showed almost
the same periodical decreasing and increasing trends as NDVI and TWSA, except that the third turning point occurred in
2010 rather than 2011. Linear regression gave a coefficient of determination $R^2=0.59$ ($p=0.002$) between annual TWSA and
NDVI, higher than that between TWSA and GPP ($R^2=0.12$, $p=0.257$), which may imply a more direct and stronger impact of
170 water stress on vegetation greenness than productivity at an annual scale.

3.3 Interactions between hydroclimate and vegetation

Combining Fig. 2-5, we found that climate condition, water storage and vegetation dynamics are tightly interlinked.
Coefficient of determination between anomalies of these variables (Fig. 6) show that variation of annual NDVI can be
explained by TWS by 58.6% ($p=0.002$), followed by P (35.9%, $p=0.031$) and AI (15.0%, $p=0.191$). Influence of these three
175 variables on GPP followed the same order ($R^2=0.12$, 0.09, 0.02) but not statistically significant ($p>0.05$). In addition, GPP
was positively associated with NDVI ($R^2=0.17$, $p=0.163$), and P and TWS were negatively correlated with dryness.

Spatially, precipitation, water storage and dryness affected vegetation in a similar way compared to temporal characteristics,
i.e. the influence of TWS was relatively stronger than P and AI. The hotspots of the interactions were found in the middle
areas, and dryness more negatively affected greenness than productivity in these areas (Fig. 7). These analyses indicate that
180 atmospheric stress and water stress imposed more direct and stronger impact on vegetation greenness than productivity on a
yearly basis, and water constraint on vegetation was stronger than that of dryness.

At the monthly scale, however, the linear responses of GPP to P and TWS were stronger than the linear responses of NDVI
to P and TWS (Fig. 8a-b). The response of both NDVI and GPP to P was more nonlinear than to TWS, and the sensitivity of
NDVI and GPP to TWS was stronger than to P indicated by the regression slopes, implying a stronger link between water
185 storage and vegetation growth. Meanwhile, increase in dryness resulted in nonlinear decreases in NDVI and GPP (Fig. 8c).
The relationships show that although precipitation is the main water input to the terrestrial hydrological cycle, it is how much
water is stored in the soils that determines vegetation greenness and biomass production at a shorter time scale than annual.
Nonlinear plant-water relationships can be explained by the lag effect that monthly changes of NDVI and GPP fell behind
the changes of P and TWS to varying degrees (Fig. 9). This means that the water restriction on vegetation outweighed the
190 water consumption by vegetation. Vegetation response to hydroclimate changes is expected to differ in dry and wet years.
Here, we assumed that the annual anomalies of $TWS<0$, $NDVI<0$ and $AI>0$ corresponded to dry conditions, and hence



defined 2003, 2005, 2007, 2009 and 2011 as dry years and 2002, 2006, 2008, 2010, 2012-2014 as relatively wet years. There was evidence of drought occurrences in these dry years (Lin et al., 2017; Wang et al., 2014b). It can be seen that the dry and wet years were mainly differentiated by the rainfall data in summer months July and August affecting water storage and dryness. The range of NDVI and GPP was 32.8% and 8.4% higher on average in dry years than wet years, mainly attributable to the difference in the non-growing seasons from October to March. Both the minimum and maximum NDVI were lower in dry years than in wet years, particularly, the minimum NDVI in dry years was 87.4% lower than that in the wet years, compared to 8.6% lower for the maximum. GPP was similar in dry and wet years, with only 9.8% and 6.9% lower in dry years for minimum and maximum values, respectively. This implies that vegetation greenness is more sensitive to any changes in hydroclimate than productivity. Moreover, GPP in non-growing seasons in dry years was relatively higher than that in wet years reflecting a positive effect of stress on biomass accumulation.

Figure 10 gives the R^2 from linear regression between different variables considering phase shift for lag analysis. It shows NDVI varied strongest with P, TWSA and AI in the previous 3, 1 and 3 months, respectively when considering all data during 2002-2014. In comparison, a shorter lag time of GPP to P, TWSA, and AI was detected (2, 0, 1 month, respectively). Comparison of the lag time in dry and wet years shows that the influence of P on vegetation was more prominent in wet years than in dry years, while TWS influence was greater in dry years than wet years. Moreover, NDVI responded faster to dryness change in dry years (2 months) than wet years (3 months), and GPP responded slower to dryness change in dry years (1 month) than wet years (0 month). This may indicate that dryness can stimulate biomass production to some degree. In addition, GPP varied synchronously with TWS showing a high dependency on water storage despite the dryness conditions.

210 4 Discussion

4.1 Uncertainties in the datasets and results

Data availability is one of the greatest obstacles for large-scale and long-term ecohydrological studies. Remote sensing products are thus useful to characterize ecohydrological changes in a large sparsely monitored basin. In this study, we used remote sensing and assimilated data of water storage, vegetation status and precipitation to assess their relationships. GLDAS uses meteorological forcing data merged from multiple sources including ground and satellite observations, and GLDAS precipitation proves to be highly consistent with observations in China (Mo et al., 2016; Wang et al., 2016). Here we also compared the GLDAS P with the measured P in the pixels where stations are available (Fig. 11). Overall, P from GLDAS agreed well with observations with R^2 ranging from 0.69 to 0.89 (± 0.05) spatially, while on average the monthly P from GLDAS underestimated observations by ~10% over all valid pixels. The comparison provides some confidence in applying the GLDAS products for long-term hydrological trend analysis, though discrepancies exist in the absolute values. Regarding the water storage change, the distribution and magnitude in the middle and lower reaches of the basin was similar to the results in Luo et al. (2016), but the increasing trends of TWS were detected in the upland opposite to their study. This



could be attributable to firstly that they used 1° GRACE data (release-5) during 2003-11/2014 and we used 0.5° data (release-6) during 04/2002-03/2015, and secondly the way the annual values were calculated: we used the hydrological year (i.e. April to March of next year) instead of the calendar year. In addition to this study and Luo et al. (2016), Zhao et al. (2011) found an overall significant increase of 9.2 mm yr⁻¹ in TWS using 1° GRACE data during 02/2003-02/2009; Mo et al. (2016) detected also a significant increase of TWS by 5.5 mm yr⁻¹ using 1° GRACE data during 2003-2013; Long et al. (2017) used the 0.5° GRACE data (release-6) for TWS analysis and found a significant increase trend of 6.3 mm yr⁻¹ during 04/2002-03/2015. It is thus important to consider the data source, spatial resolution and temporal coverage (due to interannual variability) when detecting the TWS trends for comparison. Nonetheless, it can be concluded that TWS in the PRB has been steadily increasing from the early 2000s at a rate of ~6 mm yr⁻¹.

GPP data from MODIS have been extensively used in literature to facilitate studies of vegetation in response to climate and hydrology. For example, A et al. (2017) discussed the relationship between TWS, soil moisture and GPP in response to drought in 2011 in Texas, USA, and found that vegetation dependency on TWS weakened in the shrub-dominated west and strengthened in the grassland and forest area. Liu et al. (2014c) compared five GPP datasets against observations at six sites across China and concluded that MODIS GPP was more reliable over grassland, cropland and mixed forestland than the other datasets. These land cover types happen to be the predominant ones in the Pearl River Basin. Zhang et al. (2017b) and Yuan et al. (2015) also compared various GPP datasets globally and regionally, and inconsistencies existed in these comparisons that could stem from the way each algorithm parameterizing atmospheric and water stress and difference in the vegetation index data (Yuan et al., 2015). Despite the dispute of data accuracy, MODIS GPP seems more frequently used due to its moderate spatiotemporal resolution and data coverage.

Inspired by the studies of TWS change using GRACE satellite data with different processing algorithms (Long et al., 2017; Sakumura et al., 2014), it may be more accurate and informative by using the average values from as many available datasets for the targeted ecohydrological variables as possible, i.e. the ensemble means, than using a single dataset. This is worth further investigation which could enhance the studies in many ungauged basins for critical hydrological assessments.

4.2 Hotspot for hydroclimate and vegetation changes

NDVI and GPP shared the same spatial patterns and high GPP corresponded to high NDVI in the forested areas. Low values existed in the west upland with grass cover and the central south areas of croplands. Over the 13 years NDVI and GPP showed insignificant changes with large interannual variabilities. Unlike the north China where vegetation cover is deeply affected and largely recovered through decades of ecological restoration projects (Chen et al., 2019; Feng et al., 2005), vegetation cover especially the forest cover which occupies most of the PRB almost remained constant from early 2000s (Chen et al., 2015). Even so, we identified the areas with significant increase in NDVI and GPP in the central south region of the basin where croplands dominate. Therefore, considering that the precipitation gradually decreases from southeast coastal area toward northwest outback of the basin, changes of TWS, NDVI and GPP jointly imply that the water storage increase in this hotspot region has resulted in the intensification of agricultural activities and boosted the food production since the early



2000s. It is for the first time in studies to reveal such phenomenon and can be meaningful for the food-water nexus studies in this region, and informative for a possible shift of China's main food production from the north to the south in the context of water richness in the south and shortages in the north (Kuang et al., 2015).

4.3 Causal roles of water and dryness in vegetation changes

260 The overall TWS increase is promising for the managers and users of water resources in the PRB, however, the strong correlation with precipitation seasonality restrained the available water in the relatively dry periods. In fact, previous studies have reported the contribution and restriction of P to TWS. For instance, Chen et al. (2017) revealed the liability of P to TWS ($r=0.78$) in the PRB. Mo et al. (2016) found TWS more strongly explained (60%) by annual P in river basins in south China than in north China. In this sense, storage shortage in dry periods subject to seasonal reduction of precipitation would
265 hamper vegetation growth. Analysis in this study shows that NDVI was highly correlated with TWS and P at the annual scale (Fig. 6), consistent with previous studies in the PRB and other areas (Guan et al., 2015; Zhaos et al., 2016; Zhu et al., 2018). Whilst at the monthly scale NDVI was still strongly influenced by TWS but not by P, in comparison to the strong response of GPP to both P and TWS. The weakened linear influence of P on NDVI at the monthly scale, found also by others such as Bai et al. (2019) and A et al. (2017), can be explained by the lag effect that NDVI lagged by 3 and 1 months
270 after P and TWS, respectively. In comparison, the lag time between GPP, P and TWS was 1 month shorter than NDVI versus P and TWS. In addition, comparison of the plant-water relations in dry and wet years showed a slower response of GPP to aridity index in dry years than wet years (Fig. 10b-c), which may imply that a certain degree of drying can stimulate biomass accumulation. This phenomenon is similar to the principle of regulated irrigation in agriculture to increase water use efficiency under a certain degree of water stress (Chai et al., 2016), and also revealed by other studies (Zhang and Zhang,
275 2019). This dryness effect on ecosystem productivity cannot be detected in the annual scale assessment (Brookshire and Weaver, 2015; Yao et al., 2020). These results indicate firstly that pre-growing season hydroclimate conditions play a key role in the follow-on vegetation growth and production (Wang et al., 2019), and secondly that water limits vegetation even in this subtropical rain-abundant region instead of water shortage resulted from vegetation establishment.

Anomalies of TWS, aridity index and NDVI together well defined the occurrences of drought in the basin that are identical
280 to other studies using P, TWS alone or other drought indices (Wang et al., 2014b; Zhang et al., 2018). The drying episodes confined the vegetation greenness and production (Lin et al., 2017). Liu et al. (2014b) reported that China's national total annual net ecosystem productivity exhibited declines during 2000-2011, mainly due to the reduction in GPP caused by extensive drought. Although drought is generally associated with declines in vegetation greenness and productivity due to water and heat stresses (Eamus et al., 2013), the magnitude of vegetation reduction, determined by ecosystem sensitivity to
285 drought, can vary dramatically across plant communities. While Zhang et al. (2017a) detected insensitivity of vegetation to droughts in humid south China including the lower reach of PRB, this study observed that NDVI experienced a recovery in 2004 after drought in the previous year, which may be a result of irrigation during drought in the agricultural regions since forests are more resilient to droughts (DeSoto et al., 2020; Fang and Zhang, 2019). Future climate projections predict



increases in temperature and insignificant changes in precipitation in the basin which would trigger more heatwave induced
290 flash droughts (Li et al., 2020). To mitigate the impacts on both water resources and ecosystems, proper plans should be
made such as conversion of the low resilient ecosystems to forests (Fang and Zhang, 2019) and improvement of biodiversity
in ecosystems (Isbell et al., 2015; Oliver et al., 2015), in addition to engineering regulations like reservoir operations (Lin et
al., 2017).

5 Conclusions

295 Plant-water relations over the Pearl River Basin were examined using remote sensing products during the hydrological years
of 2002-2014. Results show that water storage has increased across the entire basin at an average rate of 5.9 mm yr⁻¹.
Vegetation greenness and productivity has also shown some changes but not overall significant. Spatial characterization
reveals that the central south areas of the basin dominated by croplands are the hotspots for the changes of and interactions
between hydroclimate and vegetation. This implies an increase in food production induced by intensification of agricultural
300 activities in these areas. Lag effect analysis at the monthly scale reflects that even in this rain-abundant subtropical basin the
water restriction on vegetation precedes the water consumption by vegetation. Furthermore, comparison of the plant-water
relations in dry and wet years showed a stronger influence of precipitation and a weaker influence of water storage on
vegetation in wet years than dry years. A slower response of vegetation productivity to aridity index in dry years than wet
years was identified which may indicate a stimulating role of a certain degree of dryness on vegetation production. This
305 study reveals the changes and interplay between plant and water using readily available remote sensing and assimilated data,
and has implications for proper measures regarding land use alterations to mitigating frequent drought impacts on water
resources and ecosystems under a warming climate.

Data availability

The original data in the study are available from the links given in Table 1; the processed data can be obtained from the
310 corresponding author on request.

Author contribution

Wang: Conceptualization, Methodology, Writing – original draft; Duan: Methodology, Writing – review & editing; Liu &
Chen: Writing – review & editing, Validation.

Competing interests

315 The authors declare that they have no conflict of interest.



Acknowledgements

This work is supported by the Guangdong Provincial Department of Science and Technology, China (2019ZT08G090), and the Open Research Fund of State Key Laboratory of Simulation and Regulation of Water Cycle in River Basin, China (IWHR-SKL-201920), and the National Natural Science Foundation of China, China (51909285).

320 References

- A, G., Velicogna, I., Kimball, J. S., Du, J., Kim, Y., Colliander, A. and Njoku, E.: Satellite-observed changes in vegetation sensitivities to surface soil moisture and total water storage variations since the 2011 Texas drought, *Environ. Res. Lett.*, 12(5), doi:10.1088/1748-9326/aa6965, 2017.
- Adhami, M., Sadeghi, S. H., Duttman, R. and Sheikhmohammady, M.: Changes in watershed hydrological behavior due to land use comanagement scenarios, *J. Hydrol.*, 577, 124001, doi:10.1016/j.jhydrol.2019.124001, 2019.
- 325 Aranda, I., Forner, A., Cuesta, B. and Valladares, F.: Species-specific water use by forest tree species: From the tree to the stand, *Agric. Water Manag.*, 114, 67–77, doi:10.1016/j.agwat.2012.06.024, 2012.
- Bai, J., Shi, H., Yu, Q., Xie, Z., Li, L., Luo, G., Jin, N. and Li, J.: Satellite-observed vegetation stability in response to changes in climate and total water storage in Central Asia, *Sci. Total Environ.*, 659, 862–871, doi:10.1016/j.scitotenv.2018.12.418, 2019.
- 330 Blaschke, P., Hicks, D. and Meister, A.: Quantification of the Flood and Erosion Reduction Benefits, and Costs, of Climate Change Mitigation Measures in New Zealand, Wellington. [online] Available from: www.mfe.govt.nz (Accessed 27 April 2020), 2008.
- Brookshire, E. N. J. and Weaver, T.: Long-term decline in grassland productivity driven by increasing dryness, *Nat. Commun.*, 6(May), 1–7, doi:10.1038/ncomms8148, 2015.
- 335 Brown, A. E., Zhang, L., McMahon, T. A., Western, A. W. and Vertessy, R. A.: A review of paired catchment studies for determining changes in water yield resulting from alterations in vegetation, *J. Hydrol.*, 310(1–4), 28–61, doi:10.1016/j.jhydrol.2004.12.010, 2005.
- Chai, Q., Gan, Y., Zhao, C., Xu, H. L., Waskom, R. M., Niu, Y. and Siddique, K. H. M.: Regulated deficit irrigation for crop production under drought stress. A review, *Agron. Sustain. Dev.*, 36(1), 1–21, doi:10.1007/s13593-015-0338-6, 2016.
- 340 Chen, C., Park, T., Wang, X., Piao, S., Xu, B., Chaturvedi, R. K., Fuchs, R., Brovkin, V., Ciais, P., Fensholt, R., Tømmervik, H., Bala, G., Zhu, Z., Nemani, R. R. and Myneni, R. B.: China and India lead in greening of the world through land-use management, *Nat. Sustain.*, 2(2), 122–129, doi:10.1038/s41893-019-0220-7, 2019.
- Chen, X., Liu, X., Zhou, G., Han, L., Liu, W. and Liao, J.: 50-year evapotranspiration declining and potential causations in subtropical Guangdong province, southern China, *Catena*, 128, 185–194, doi:10.1016/j.catena.2015.02.001, 2015.
- 345



- Chen, Y. D., Zhang, Q., Xu, C. Y., Lu, X. and Zhang, S.: Multiscale streamflow variations of the Pearl River basin and possible implications for the water resource management within the Pearl River Delta, China, *Quat. Int.*, 226(1–2), 44–53, doi:10.1016/j.quaint.2009.08.014, 2010.
- Chen, Z., Jiang, W., Wu, J., Chen, K., Deng, Y., Jia, K. and Mo, X.: Detection of the spatial patterns of water storage
350 variation over China in recent 70 years, *Sci. Rep.*, 7(1), 1–9, doi:10.1038/s41598-017-06558-5, 2017.
- Deng, S., Chen, T., Yang, N., Qu, L., Li, M. and Chen, D.: Spatial and temporal distribution of rainfall and drought characteristics across the Pearl River basin, *Sci. Total Environ.*, 619–620, 28–41, doi:10.1016/j.scitotenv.2017.10.339, 2018.
- Déry, S. J. and Wood, E. F.: Decreasing river discharge in northern Canada, *Geophys. Res. Lett.*, 32(10), 1–4, doi:10.1029/2005GL022845, 2005.
- 355 DeSoto, L., Cailleret, M., Sterck, F., Jansen, S., Kramer, K., Robert, E. M. R., Aakala, T., Amoroso, M. M., Bigler, C., Camarero, J. J., Čufar, K., Gea-Izquierdo, G., Gillner, S., Haavik, L. J., Hereş, A. M., Kane, J. M., Kharuk, V. I., Kitzberger, T., Klein, T., Levanič, T., Linares, J. C., Mäkinen, H., Oberhuber, W., Papadopoulos, A., Rohner, B., Sangüesa-Barreda, G., Stojanovic, D. B., Suárez, M. L., Villalba, R. and Martínez-Vilalta, J.: Low growth resilience to drought is related to future mortality risk in trees, *Nat. Commun.*, 11(1), 1–9, doi:10.1038/s41467-020-14300-5, 2020.
- 360 Eamus, D. and Froend, R.: Groundwater-dependent ecosystems: The where, what and why of GDEs, *Aust. J. Bot.*, 54(2), 91–96, doi:10.1071/BT06029, 2006.
- Eamus, D., Boulain, N., Cleverly, J. and Breshears, D. D.: Global change-type drought-induced tree mortality: Vapor pressure deficit is more important than temperature per se in causing decline in tree health, *Ecol. Evol.*, 3(8), 2711–2729, doi:10.1002/ece3.664, 2013.
- 365 Fang, O. and Zhang, Q. Bin: Tree resilience to drought increases in the Tibetan Plateau, *Glob. Chang. Biol.*, 25(1), 245–253, doi:10.1111/gcb.14470, 2019.
- Feng, Z., Yang, Y., Zhang, Y., Zhang, P. and Li, Y.: Grain-for-green policy and its impacts on grain supply in West China, *Land use policy*, 22(4), 301–312, doi:10.1016/j.landusepol.2004.05.004, 2005.
- Fowler, M. D., Kooperman, G. J., Randerson, J. T. and Pritchard, M. S.: The effect of plant physiological responses to rising
370 CO₂ on global streamflow, *Nat. Clim. Chang.*, 9(11), 873–879, doi:10.1038/s41558-019-0602-x, 2019.
- Ghestem, M., Sidle, R. C. and Stokes, A.: The Influence of Plant Root Systems on Subsurface Flow: Implications for Slope Stability, *Bioscience*, 61(11), 869–879, doi:10.1525/bio.2011.61.11.6, 2011.
- Guan, K., Pan, M., Li, H., Wolf, A., Wu, J., Medvigy, D., Caylor, K. K., Sheffield, J., Wood, E. F., Malhi, Y., Liang, M., Kimball, J. S., Saleska, S. R., Berry, J., Joiner, J. and Lyapustin, A. I.: Photosynthetic seasonality of global tropical forests
375 constrained by hydroclimate, *Nat. Geosci.*, 8(4), 284–289, doi:10.1038/ngeo2382, 2015.
- Güsewell, S., Furrer, R., Gehrig, R. and Pietragalla, B.: Changes in temperature sensitivity of spring phenology with recent climate warming in Switzerland are related to shifts of the pre-season, *Glob. Chang. Biol.*, 23(12), 5189–5202, doi:10.1111/gcb.13781, 2017.



- Huang, L. and Zhang, Z.: Effect of rainfall pulses on plant growth and transpiration of two xerophytic shrubs in a revegetated desert area: Tengger Desert, China, *Catena*, 137, 269–276, doi:10.1016/j.catena.2015.09.020, 2015.
- Hwang, T., Martin, K. L., Vose, J. M., Wear, D., Miles, B., Kim, Y. and Band, L. E.: Nonstationary Hydrologic Behavior in Forested Watersheds Is Mediated by Climate-Induced Changes in Growing Season Length and Subsequent Vegetation Growth, *Water Resour. Res.*, 54(8), 5359–5375, doi:10.1029/2017WR022279, 2018.
- Isbell, F., Craven, D., Connolly, J., Loreau, M., Schmid, B., Beierkuhnlein, C., Bezemer, T. M., Bonin, C., Bruelheide, H., De Luca, E., Ebeling, A., Griffin, J. N., Guo, Q., Hautier, Y., Hector, A., Jentsch, A., Kreyling, J., Lanta, V., Manning, P., Meyer, S. T., Mori, A. S., Naeem, S., Niklaus, P. A., Polley, H. W., Reich, P. B., Roscher, C., Seabloom, E. W., Smith, M. D., Thakur, M. P., Tilman, D., Tracy, B. F., Van Der Putten, W. H., Van Ruijven, J., Weigelt, A., Weisser, W. W., Wilsey, B. and Eisenhauer, N.: Biodiversity increases the resistance of ecosystem productivity to climate extremes, *Nature*, 526(7574), 574–577, doi:10.1038/nature15374, 2015.
- Kuang, W., Hu, Y., Dai, X. and Song, X.: Investigation of changes in water resources and grain production in China: changing patterns and uncertainties, *Theor. Appl. Climatol.*, 122(3–4), 557–565, doi:10.1007/s00704-014-1315-8, 2015.
- Li, J., Wang, Z., Wu, X., Guo, S. and Chen, X.: Flash droughts in the Pearl River Basin, China: Observed characteristics and future changes, *Sci. Total Environ.*, 707, 136074, doi:10.1016/j.scitotenv.2019.136074, 2020.
- Liang, W., Bai, D., Wang, F., Fu, B., Yan, J., Wang, S., Yang, Y., Long, D. and Feng, M.: Quantifying the impacts of climate change and ecological restoration on streamflow changes based on a Budyko hydrological model in China's Loess Plateau, *Water Resour. Res.*, 51(8), 6500–6519, doi:10.1002/2014WR016589, 2015.
- Lin, Q., Wu, Z., Singh, V. P., Sadeghi, S. H. R., He, H. and Lu, G.: Correlation between hydrological drought, climatic factors, reservoir operation, and vegetation cover in the Xijiang Basin, South China, *J. Hydrol.*, 549, 512–524, doi:10.1016/j.jhydrol.2017.04.020, 2017.
- Liu, B., Zhao, W., Wen, Z. and Zhang, Z.: Response of water and energy exchange to the environmental variable in a desert-oasis wetland of Northwest China, *Hydrol. Process.*, 28(25), 6098–6112, doi:10.1002/hyp.10098, 2014a.
- Liu, B., Peng, S., Liao, Y. and Wang, H.: The characteristics and causes of increasingly severe saltwater intrusion in Pearl River Estuary, *Estuar. Coast. Shelf Sci.*, 220, 54–63, doi:10.1016/j.ecss.2019.02.041, 2019.
- Liu, Y., Zhou, Y., Ju, W., Wang, S., Wu, X., He, M. and Zhu, G.: Impacts of droughts on carbon sequestration by China's terrestrial ecosystems from 2000 to 2011, *Biogeosciences*, doi:10.5194/bg-11-2583-2014, 2014b.
- Liu, Z., Wang, L. and Wang, S.: Comparison of different GPP models in China using MODIS image and ChinaFLUX data, *Remote Sens.*, 6(10), 10215–10231, doi:10.3390/rs61010215, 2014c.
- Long, D., Pan, Y., Zhou, J., Chen, Y., Hou, X., Hong, Y., Scanlon, B. R. and Longuevergne, L.: Global analysis of spatiotemporal variability in merged total water storage changes using multiple GRACE products and global hydrological models, *Remote Sens. Environ.*, 192, 198–216, doi:10.1016/j.rse.2017.02.011, 2017.
- Luo, Z., Yao, C., Li, Q. and Huang, Z.: Terrestrial water storage changes over the Pearl River Basin from GRACE and connections with Pacific climate variability, *Geod. Geodyn.*, 7(3), 171–179, doi:10.1016/j.geog.2016.04.008, 2016.



- Ma, X., Huete, A., Moran, S., Ponce-Campos, G. and Eamus, D.: Abrupt shifts in phenology and vegetation productivity under climate extremes, *J. Geophys. Res. Biogeosciences*, 120(10), 2036–2052, doi:10.1002/2015JG003144, 2015.
- 415 Martin-StPaul, N., Delzon, S. and Cochard, H. H.: Plant resistance to drought depends on timely stomatal closure, edited by H. Maherali, *Ecol. Lett.*, 20(11), 1437–1447, doi:10.1111/ele.12851, 2017.
- Marvel, K., Cook, B. I., Bonfils, C. J. W., Durack, P. J., Smerdon, J. E. and Williams, A. P.: Twentieth-century hydroclimate changes consistent with human influence, *Nature*, 569(7754), 59–65, doi:10.1038/s41586-019-1149-8, 2019.
- Massmann, A., Gentine, P. and Lin, C.: When does vapor pressure deficit drive or reduce evapotranspiration?, *Hydrol. Earth*
420 *Syst. Sci. Discuss.*, doi:10.5194/hess-2018-553, 2018.
- Mo, X., Wu, J. J., Wang, Q. and Zhou, H.: Variations in water storage in China over recent decades from GRACE observations and GLDAS, *Nat. Hazards Earth Syst. Sci.*, 16(2), 469–482, doi:10.5194/nhess-16-469-2016, 2016.
- Notaro, M., Vavrus, S. and Liu, Z.: Global vegetation and climate change due to future increases in CO₂ as projected by a fully coupled model with dynamic vegetation, *J. Clim.*, 20(1), 70–90, doi:10.1175/JCLI3989.1, 2007.
- 425 Novák, V., Hortalová, T. and Matejka, F.: Predicting the effects of soil water content and soil water potential on transpiration of maize, *Agric. Water Manag.*, 76(3), 211–223, doi:10.1016/j.agwat.2005.01.009, 2005.
- Oliver, T. H., Heard, M. S., Isaac, N. J. B., Roy, D. B., Procter, D., Eigenbrod, F., Freckleton, R., Hector, A., Orme, C. D. L., Petchey, O. L., Proença, V., Raffaelli, D., Suttle, K. B., Mace, G. M., Martín-López, B., Woodcock, B. A. and Bullock, J. M.: Biodiversity and Resilience of Ecosystem Functions, *Trends Ecol. Evol.*, 30(11), 673–684, doi:10.1016/j.tree.2015.08.009,
430 2015.
- Pal, I. and Al-Tabbaa, A.: Trends in seasonal precipitation extremes - An indicator of “climate change” in Kerala, India, *J. Hydrol.*, 367(1–2), 62–69, doi:10.1016/j.jhydrol.2008.12.025, 2009.
- Petr, M., Boerboom, L. G. J., Ray, D. and Van Der Veen, A.: Adapting Scotland’s forests to climate change using an action expiration chart, *Environ. Res. Lett.*, 10(10), 105005, doi:10.1088/1748-9326/10/10/105005, 2015.
- 435 Pham-Duc, B., Papa, F., Prigent, C., Aires, F., Biancamaria, S. and Frappart, F.: Variations of surface and subsurface water storage in the Lower Mekong Basin (Vietnam and Cambodia) from multisatellite observations, *Water (Switzerland)*, 11(1), 75, doi:10.3390/w11010075, 2019.
- Plaut, J. A., Wadsworth, W. D., Pangle, R., Yepez, E. A., McDowell, N. G. and Pockman, W. T.: Reduced transpiration response to precipitation pulses precedes mortality, *New Phytol.* 2013, 200(2), 375–387, 2013.
- 440 Reyer, C. P. O., Leuzinger, S., Rammig, A., Wolf, A., Bartholomeus, R. P., Bonfante, A., de Lorenzi, F., Dury, M., Gloning, P., Abou Jaoudé, R., Klein, T., Kuster, T. M., Martins, M., Niedrist, G., Riccardi, M., Wohlfahrt, G., de Angelis, P., de Dato, G., François, L., Menzel, A. and Pereira, M.: A plant’s perspective of extremes: Terrestrial plant responses to changing climatic variability, *Glob. Chang. Biol.*, 19(1), 75–89, doi:10.1111/gcb.12023, 2013.
- Rodell, M., Houser, P. R., Jambor, U., Gottschalck, J., Mitchell, K., Meng, C. J., Arsenault, K., Cosgrove, B., Radakovich, J.,
445 Bosilovich, M., Entin, J. K., Walker, J. P., Lohmann, D. and Toll, D.: The Global Land Data Assimilation System, *Bull. Am. Meteorol. Soc.*, doi:10.1175/BAMS-85-3-381, 2004.



- Running, S. W., Heinsch, F. A., Zhao, M., Reeves, M., Hashimoto, H. and Nemani, R. R.: A Continuous Satellite-Derived Measure of Global Terrestrial Primary Production., *Bioscience*, 2004.
- Sakumura, C., Bettadpur, S. and Bruinsma, S.: Ensemble prediction and intercomparison analysis of GRACE time-variable gravity field models, *Geophys. Res. Lett.*, 41(5), 1389–1397, doi:10.1002/2013GL058632, 2014.
- 450 Sala, A., Piper, F. and Hoch, G.: Physiological mechanisms of drought-induced tree mortality are far from being resolved, *New Phytol.*, 186(2), 274–281, doi:10.1111/j.1469-8137.2009.03167.x, 2010.
- Schwärzel, K., Zhang, L., Montanarella, L., Wang, Y. and Sun, G.: How afforestation affects the water cycle in drylands: A process-based comparative analysis, *Glob. Chang. Biol.*, 26(2), 944–959, doi:10.1111/gcb.14875, 2020.
- 455 Sippel, S., Meinshausen, N., Fischer, E. M., Székely, E. and Knutti, R.: Climate change now detectable from any single day of weather at global scale, *Nat. Clim. Chang.*, 10(1), 35–41, doi:10.1038/s41558-019-0666-7, 2020.
- Soulsby, C., Dick, J., Scheliga, B. and Tetzlaff, D.: Taming the flood—How far can we go with trees?, *Hydrol. Process.*, 31(17), 3122–3126, doi:10.1002/hyp.11226, 2017.
- Stewardson, M. J., Shang, W., Kattel, G. R. and Webb, J. A.: Environmental Water and Integrated Catchment Management, 460 in *Water for the Environment: From Policy and Science to Implementation and Management*, pp. 519–536, Elsevier Inc., 2017.
- Sussmilch, F. C. and McAdam, S. A. M.: Surviving a dry future: Abscisic acid (ABA)-mediated plant mechanisms for conserving water under low humidity, *Plants*, 6(4), doi:10.3390/plants6040054, 2017.
- Tapley, B. D., Bettadpur, S., Ries, J. C., Thompson, P. F. and Watkins, M. M.: GRACE measurements of mass variability in 465 the Earth system, *Science* (80-.), 305(5683), 503–505, doi:10.1126/science.1099192, 2004.
- Wang, H., Guan, H., Gutiérrez-Jurado, H. A. and Simmons, C. T.: Examination of water budget using satellite products over Australia, *J. Hydrol.*, 511, 546–554, doi:10.1016/j.jhydrol.2014.01.076, 2014a.
- Wang, H., Tetzlaff, D., Dick, J. J. and Soulsby, C.: Assessing the environmental controls on Scots pine transpiration and the implications for water partitioning in a boreal headwater catchment, *Agric. For. Meteorol.*, 240–241(April), 58–66, 470 doi:10.1016/j.agrformet.2017.04.002, 2017.
- Wang, H., Tetzlaff, D., Buttle, J., Carey, S. K., Laudon, H., McNamara, J. P., Spence, C. and Soulsby, C.: Climate-phenology-hydrology interactions in northern high latitudes: Assessing the value of remote sensing data in catchment ecohydrological studies, *Sci. Total Environ.*, 656, 19–28, doi:10.1016/j.scitotenv.2018.11.361, 2019.
- Wang, J., Jiang, D., Huang, Y. and Wang, H.: Drought analysis of the Haihe river basin based on GRACE terrestrial water 475 storage, *Sci. World J.*, 2014, doi:10.1155/2014/578372, 2014b.
- Wang, W., Cui, W., Wang, X. and Chen, X.: Evaluation of GLDAS-1 and GLDAS-2 forcing data and noah model simulations over China at the monthly scale, *J. Hydrometeorol.*, 17(11), 2815–2833, doi:10.1175/JHM-D-15-0191.1, 2016.
- Wang, Y., Yu, P., Xiong, W., Shen, Z., Guo, M., Shi, Z., Du, A. and Wang, L.: Water-yield reduction after afforestation and related processes in the semiarid Liupan Mountains, northwest China, *J. Am. Water Resour. Assoc.*, 44(5), 1086–1097, 480 doi:10.1111/j.1752-1688.2008.00238.x, 2008.



- Wheater, H. and Evans, E.: Land use, water management and future flood risk, *Land use policy*, 26(SUPPL. 1), doi:10.1016/j.landusepol.2009.08.019, 2009.
- Xia, Y. Q. and Shao, M. A.: Soil water carrying capacity for vegetation: A hydrologic and biogeochemical process model solution, *Ecol. Modell.*, 214(2–4), 112–124, doi:10.1016/j.ecolmodel.2008.01.024, 2008.
- 485 Xiao, J., Chevallier, F., Gomez, C., Guanter, L., Hicke, J. A., Huete, A. R., Ichii, K., Ni, W., Pang, Y., Rahman, A. F., Sun, G., Yuan, W., Zhang, L. and Zhang, X.: Remote sensing of the terrestrial carbon cycle: A review of advances over 50 years, *Remote Sens. Environ.*, 233(August), 111383, doi:10.1016/j.rse.2019.111383, 2019.
- Xu, K., Qin, G., Niu, J., Wu, C., Hu, B. X., Huang, G. and Wang, P.: Comparative analysis of meteorological and hydrological drought over the Pearl River basin in southern China, *Hydrol. Res.*, 50(1), 301–318, doi:10.2166/nh.2018.178, 490 2019.
- Xu, X., Zhang, Q., Li, Y. and Li, X.: Evaluating the influence of water table depth on transpiration of two vegetation communities in a lake floodplain wetland, *Hydrol. Res.*, 47(S1), 293–312, doi:10.2166/nh.2016.011, 2016.
- Yang, Q., Zhao, W., Liu, B. and Liu, H.: Physiological responses of *Haloxylon ammodendron* to rainfall pulses in temperate desert regions, Northwest China, *Trees - Struct. Funct.*, 28(3), 709–722, doi:10.1007/s00468-014-0983-4, 2014.
- 495 Yang, Y., Guan, H., Batelaan, O., McVicar, T. R., Long, D., Piao, S., Liang, W., Liu, B., Jin, Z. and Simmons, C. T.: Contrasting responses of water use efficiency to drought across global terrestrial ecosystems, *Sci. Rep.*, 6(March), 1–8, doi:10.1038/srep23284, 2016.
- Yao, J., Liu, H., Huang, J., Gao, Z., Wang, G., Li, D., Yu, H. and Chen, X.: Accelerated dryland expansion regulates future variability in dryland gross primary production, *Nat. Commun.*, 11(1), 1–10, doi:10.1038/s41467-020-15515-2, 2020.
- 500 Yosef, G., Walko, R., Avisar, R., Tatarinov, F., Rotenberg, E. and Yakir, D.: Large-scale semi-arid afforestation can enhance precipitation and carbon sequestration potential, *Sci. Rep.*, 8(1), 1–10, doi:10.1038/s41598-018-19265-6, 2018.
- Yu, J. and Wang, P.: Relationship between Water and Vegetation in the Ejina Delta, *Bull. Chinese Acad. Sci. BCAS*, 2012.
- Yuan, W., Cai, W., Nguy-Robertson, A. L., Fang, H., Suyker, A. E., Chen, Y., Dong, W., Liu, S. and Zhang, H.: Uncertainty in simulating gross primary production of cropland ecosystem from satellite-based models, *Agric. For. Meteorol.*, 207, 48– 505 57, doi:10.1016/j.agrformet.2015.03.016, 2015.
- Zhang, Q., Xu, C. Y. and Zhang, Z.: Observed changes of drought/wetness episodes in the Pearl River basin, China, using the standardized precipitation index and aridity index, *Theor. Appl. Climatol.*, 98(1–2), 89–99, doi:10.1007/s00704-008-0095-4, 2009.
- Zhang, Q., Kong, D., Singh, V. P. and Shi, P.: Response of vegetation to different time-scales drought across China: Spatiotemporal patterns, causes and implications, *Glob. Planet. Change*, 152, 1–11, doi:10.1016/j.gloplacha.2017.02.008, 2017a.
- Zhang, X. and Zhang, B.: The responses of natural vegetation dynamics to drought during the growing season across China, *J. Hydrol.*, 574(January), 706–714, doi:10.1016/j.jhydrol.2019.04.084, 2019.

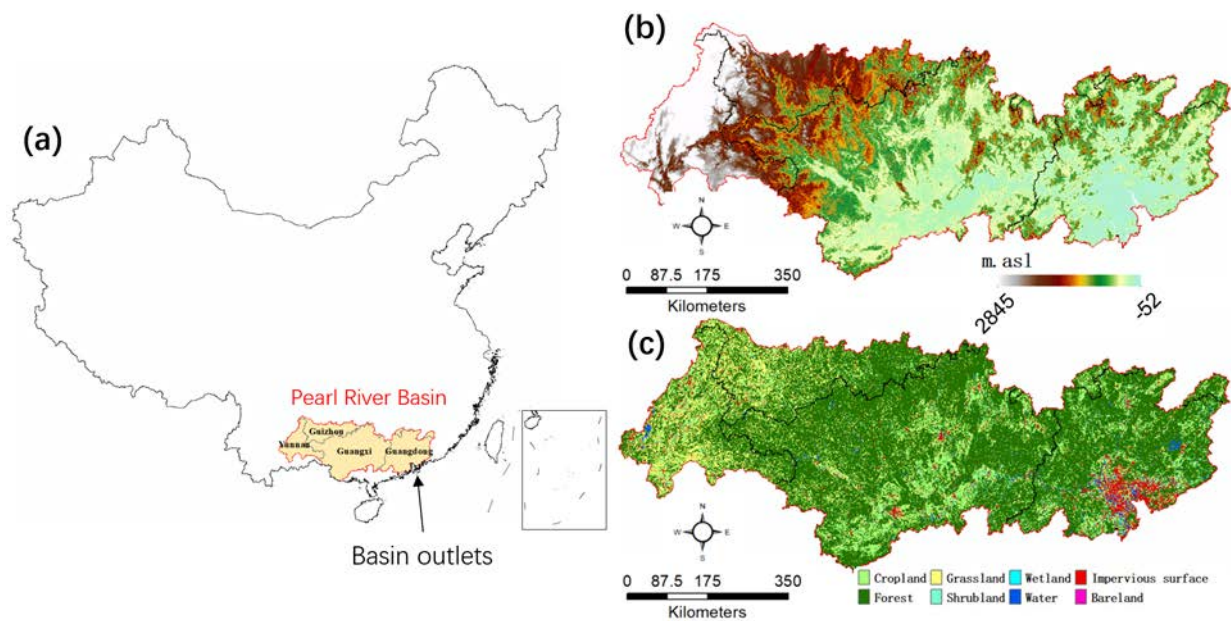


- 515 Zhang, Y., Xiao, X., Wu, X., Zhou, S., Zhang, G., Qin, Y. and Dong, J.: A global moderate resolution dataset of gross primary production of vegetation for 2000-2016, *Sci. data*, 4, 170165, doi:10.1038/sdata.2017.165, 2017b.
- Zhang, Y., Li, Y., Ge, J., Li, G., Yu, Z. and Niu, H.: Correlation analysis between drought indices and terrestrial water storage from 2002 to 2015 in China, *Environ. Earth Sci.*, 77(12), 1–12, doi:10.1007/s12665-018-7651-8, 2018.
- 520 Zhao, J., Wang, D., Yang, H. and Sivapalan, M.: Unifying catchment water balance models for different time scales through the maximum entropy production principle, *Water Resour. Res.*, 52, 7503–7512, doi:10.1002/2016WR018977. Received, 2016.
- Zhao, Q. Le, Liu, X. L., Ditmar, P., Siemes, C., Revtova, E., Hashemi-Farahani, H. and Klees, R.: Water storage variations of the Yangtze, Yellow, and Zhujiang river basins derived from the DEOS Mass Transport (DMT-1) model, *Sci. China Earth Sci.*, 54(5), 667–677, doi:10.1007/s11430-010-4096-7, 2011.
- 525 Zhao, W. and Liu, B.: The response of sap flow in shrubs to rainfall pulses in the desert region of China, *Agric. For. Meteorol.*, 150(9), 1297–1306, doi:10.1016/j.agrformet.2010.05.012, 2010.
- Zhu, B., Xie, X. and Zhang, K.: Water storage and vegetation changes in response to the 2009/10 drought over North China, *Hydrol. Res.*, 49(5), 1618–1635, doi:10.2166/nh.2018.087, 2018.



530 **Table 1.** Information of data used in this study

	Product	Resolution	Time span	Source
P, ET_p	GLDAS- Noah (v2.1)	0.25°×0.25°, Monthly	04/2002– 03/2015	https://disc.gsfc.nasa.gov
TWSA	GRACE (RL06)	0.5°×0.5°, Monthly	04/2002– 03/2015	http://grace.jpl.nasa.gov ; www2.csr.utexas.edu/grace/RL06_mascons.html
NDVI	GIMMS3g (v1)	0.083°×0.083°, 15–day	04/2002– 03/2015	https://ecocast.arc.nasa.gov/data/pub/gimms/3g.v1
GPP	MOD17A2	0.05°×0.05°, Monthly	04/2002– 03/2015	www.ntsg.umt.edu/project/modis/mod17.php



535 **Figure 1.** (a) The Pearl River Basin and the related provinces on the map of the China, (b) Digital elevation map (m.a.s.l,
1000 m resolution), and (c) Land cover types (30 m resolution).

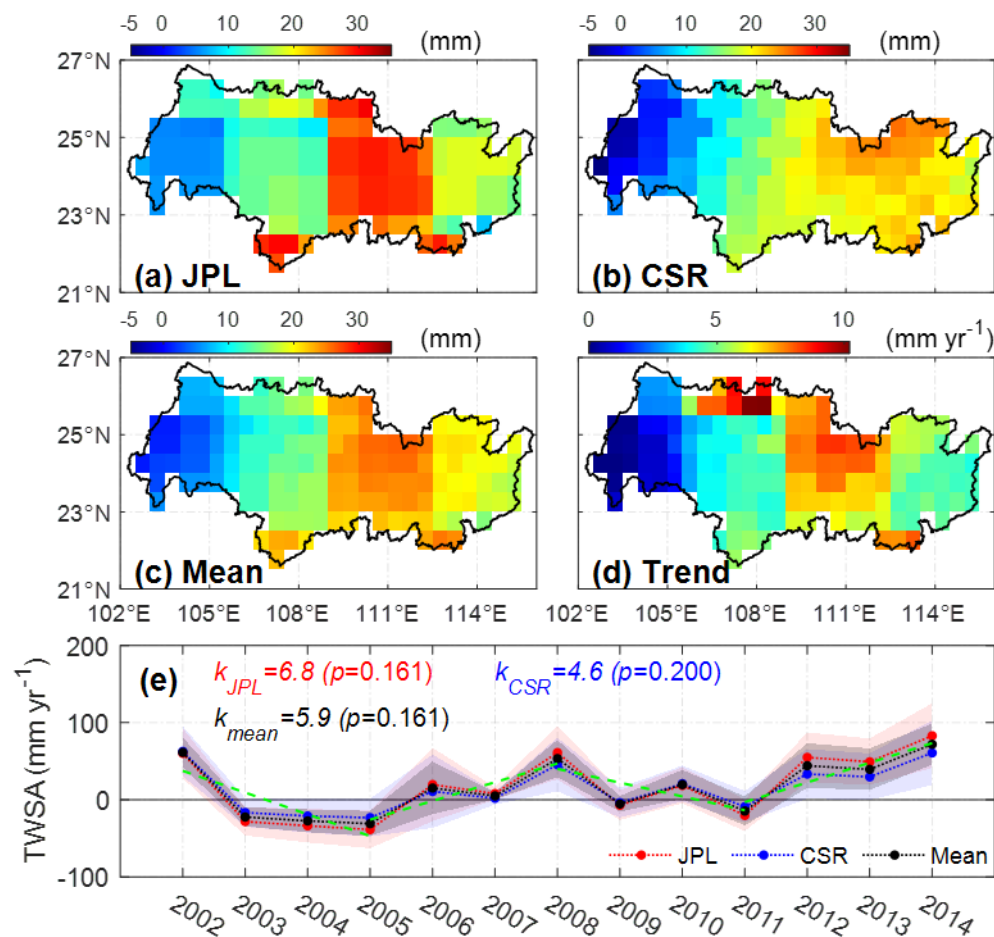
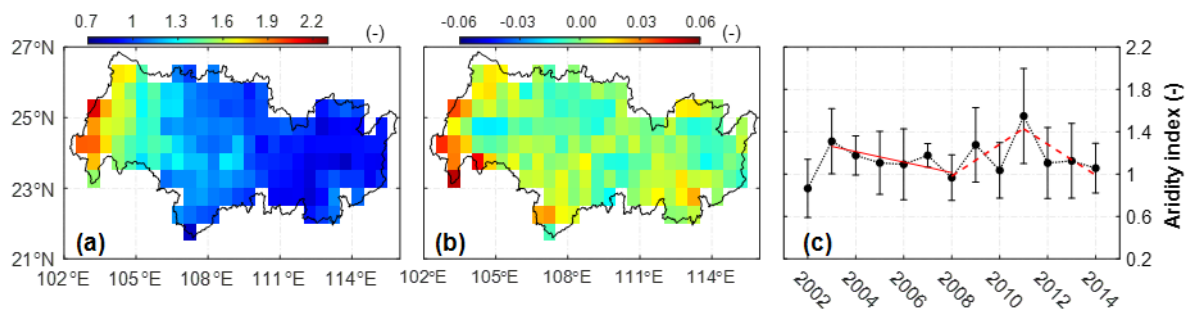
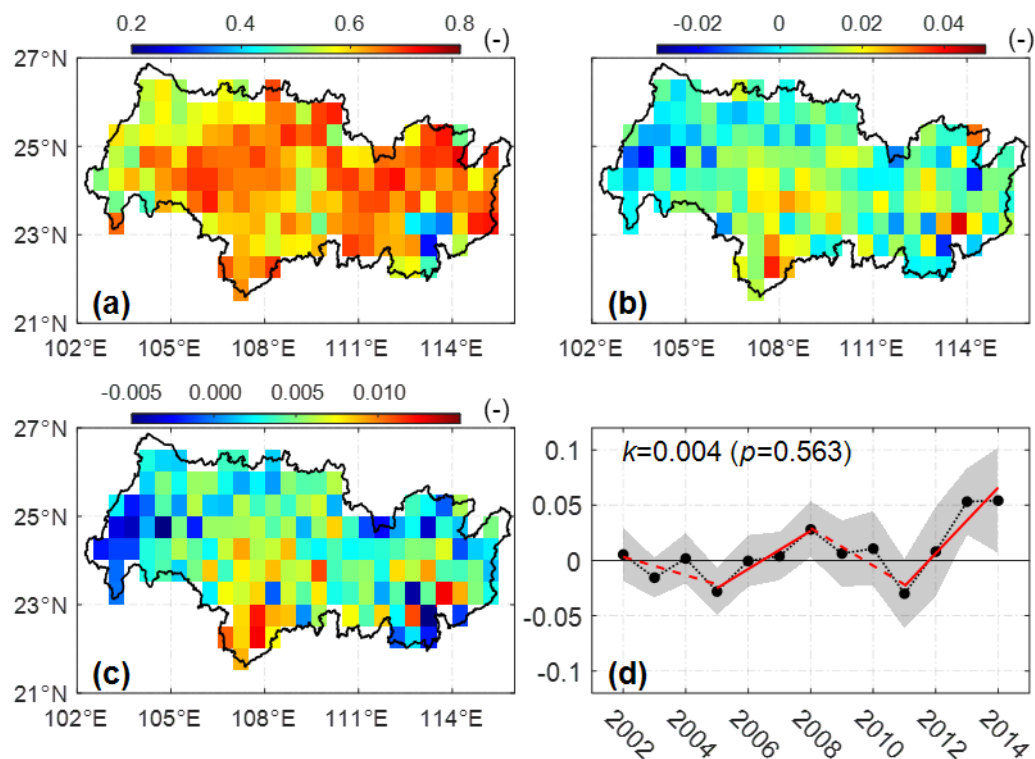


Figure 2. Spatial distribution of TWSA in the basin inferred by (a) GRACE_{JPL}, (b) GRACE_{CSR}, (c) the mean of GRACE_{JPL} and GRACE_{CSR}, (d) the linear trends of the mean annual TWSA, and (e) mean annual TWSA over the entire basin. Shaded areas in (e) show the standard error of each series. Dashed green lines indicate statistically insignificant trends ($R^2=0.68, 0.82, 0.58$ and 0.83 , respectively).

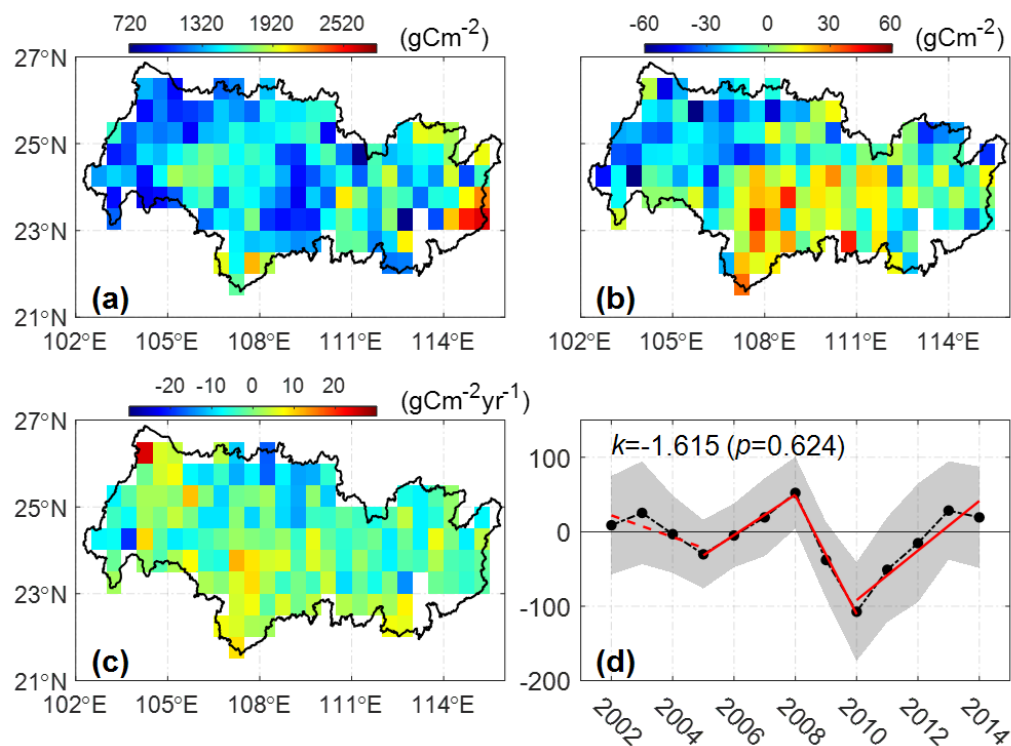
540



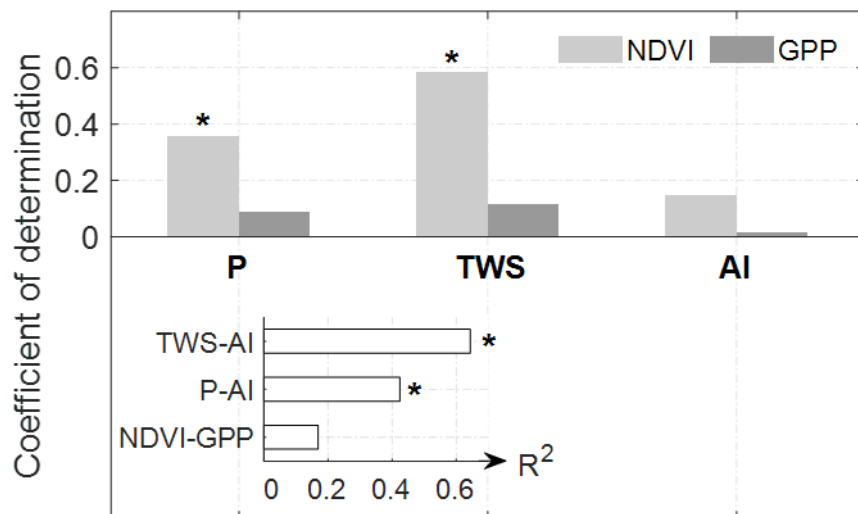
545 **Figure 3.** (a) Spatial distribution of the mean annual aridity index across the basin during hydrological years 2002-2016, (b) annual trend of aridity index, and (c) mean annual aridity index over the basin. Red lines show the periodical trends. Dashed red line indicates statistically insignificant trend. The coefficient of determination is 0.66, 0.54 and 0.68, respectively.



550 **Figure 4.** Spatial distribution of (a) mean annual NDVI, (b) mean annual NDVI anomaly, (c) linear trend of annual NDVI anomaly; and (d) spatially averaged annual NDVI anomaly, during 2002-2014. Red lines show the annual trends in different periods. Dashed red lines show statistically insignificant trends ($p>0.05$). Coefficient of determination is 0.47, 0.94, 0.81 and 0.90 for the four periods.

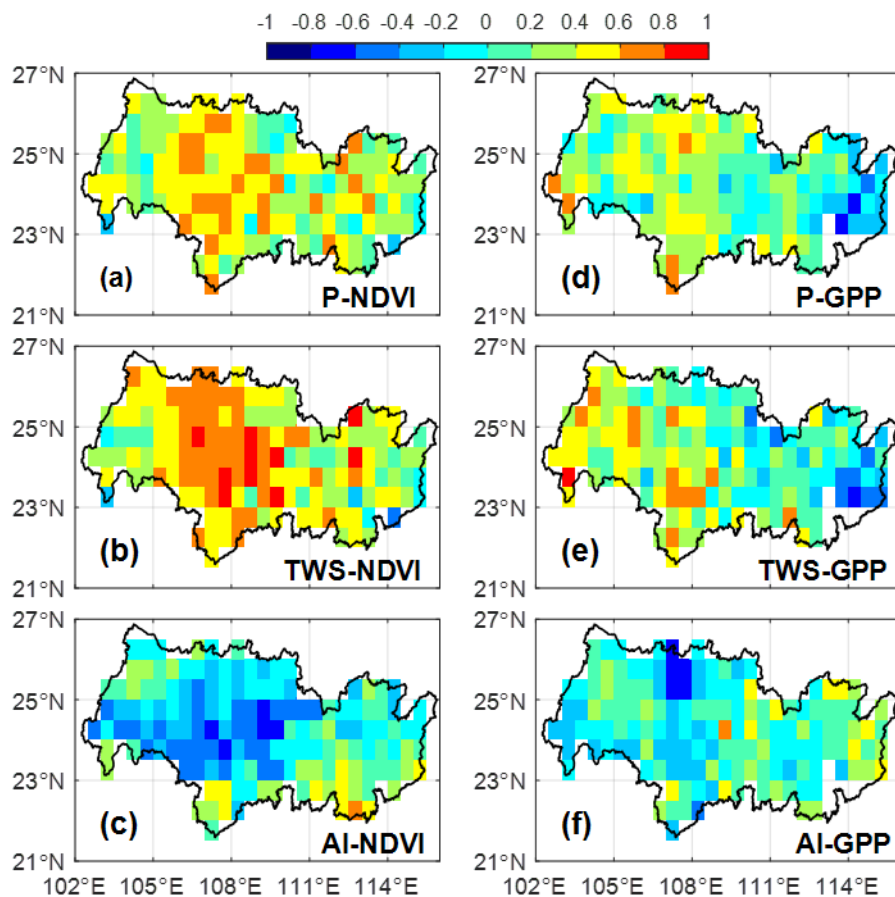


555 **Figure 5.** Spatial distribution of (a) mean annual GPP, (b) mean annual GPP anomaly, (c) linear trend of annual GPP anomaly; and (d) spatially averaged annual GPP anomaly, during 2002-2014. Red lines show the annual trends in different periods. Dashed red lines show statistically insignificant trends. The coefficient of determination is 0.65, 0.99, 0.99 and 0.90 for the four periods.

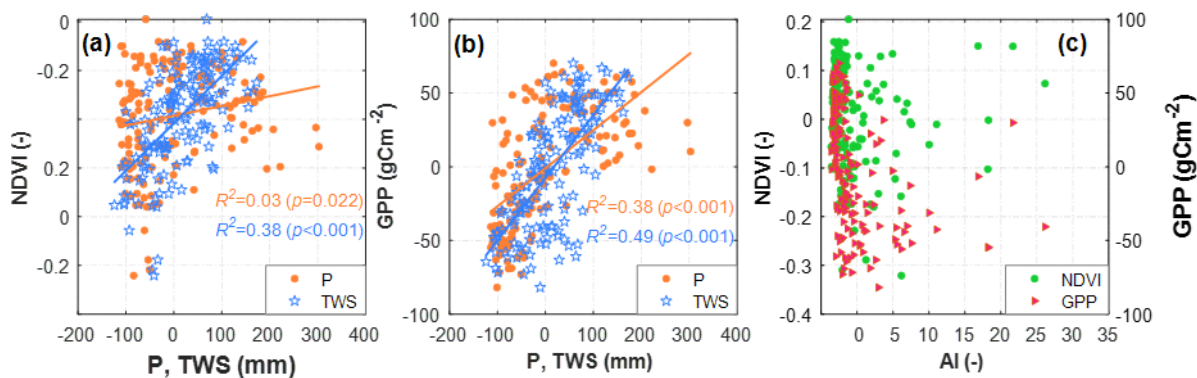


560

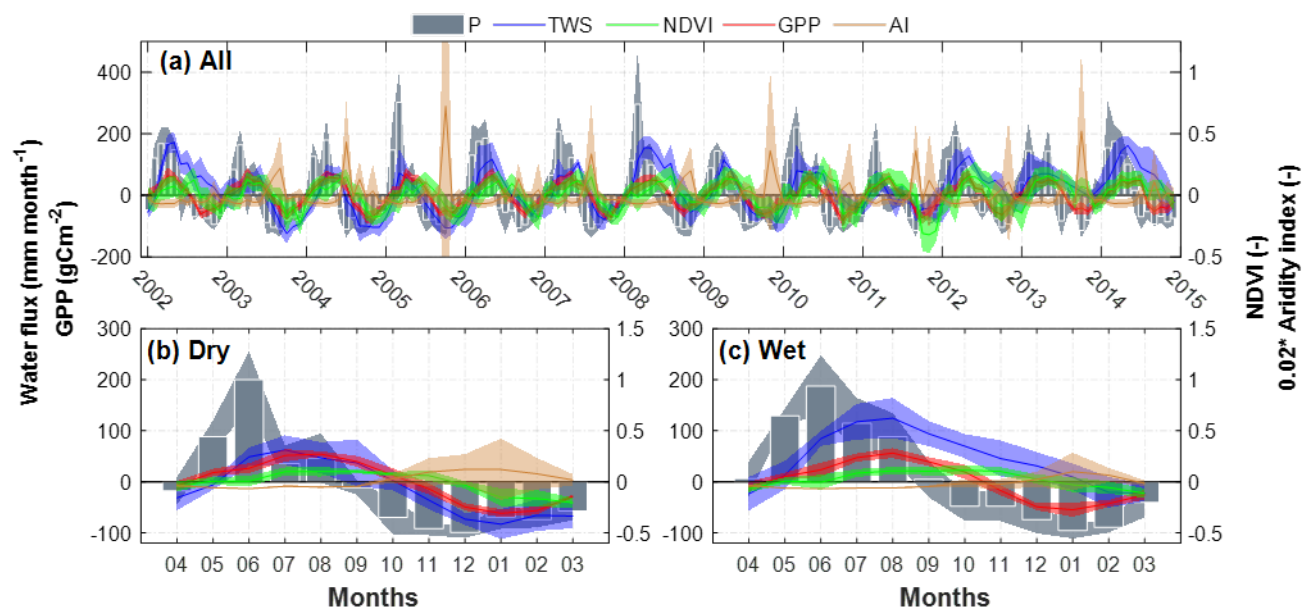
Figure 6. Coefficient of determination (R^2) from linear regressions between the anomalies of P, TWS, AI, NDVI and GPP at the annual scale. Asterisk indicates $p < 0.05$.



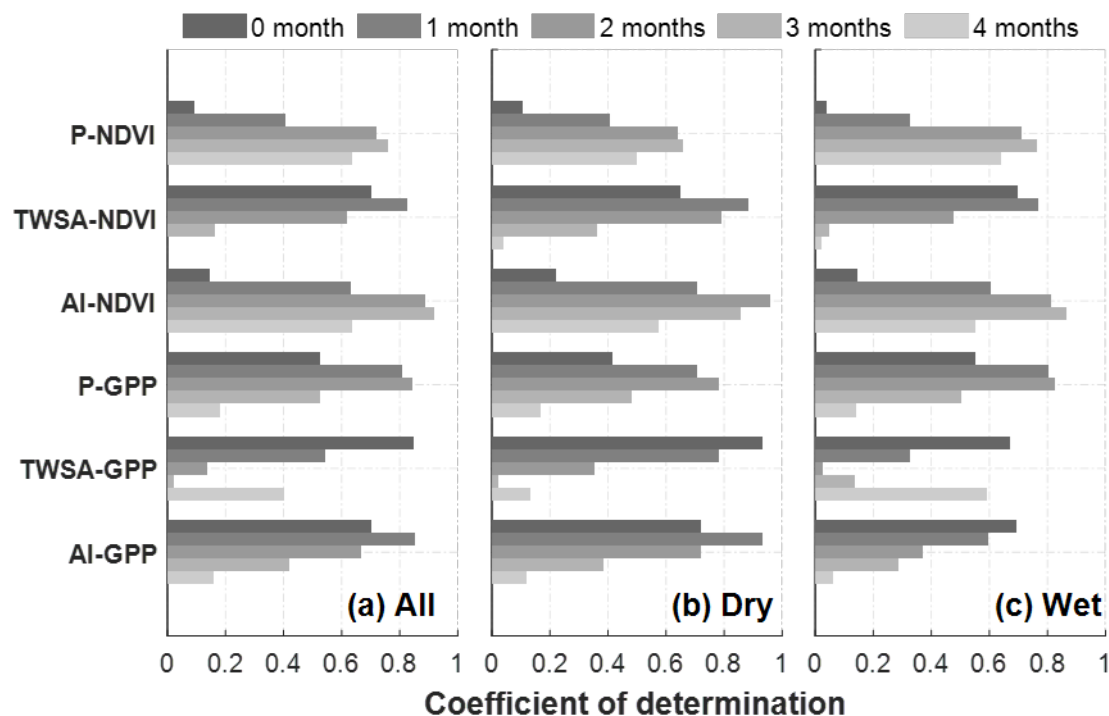
565 **Figure 7.** Pearson correlation coefficient between annual anomalies of (a-c) precipitation, total water storage, aridity index and NDVI; and (d-f) precipitation, total water storage, aridity index and GPP.



570 **Figure 8.** Scatter plot of monthly anomalies of precipitation (P), total water storage (TWS), aridity index (AI), NDVI and GPP.



575 **Figure 9.** (a) Monthly variations of anomalies of precipitation (P), total water storage (TWS), NDVI, gross primary production (GPP) and aridity index (AI, scaled for a better view) in all years; (b) monthly means of dry hydrological years and (c) monthly means of wet hydrological years during 2002-2014. Shaded areas show the standard errors of each variable.



580 **Figure 10.** Coefficient of determination between monthly anomalies of precipitation (P), total water storage (TWS), aridity index (AI) and NDVI and GPP in (a) all years, (b) the dry years, and (c) the wet years after shifting different number of months.

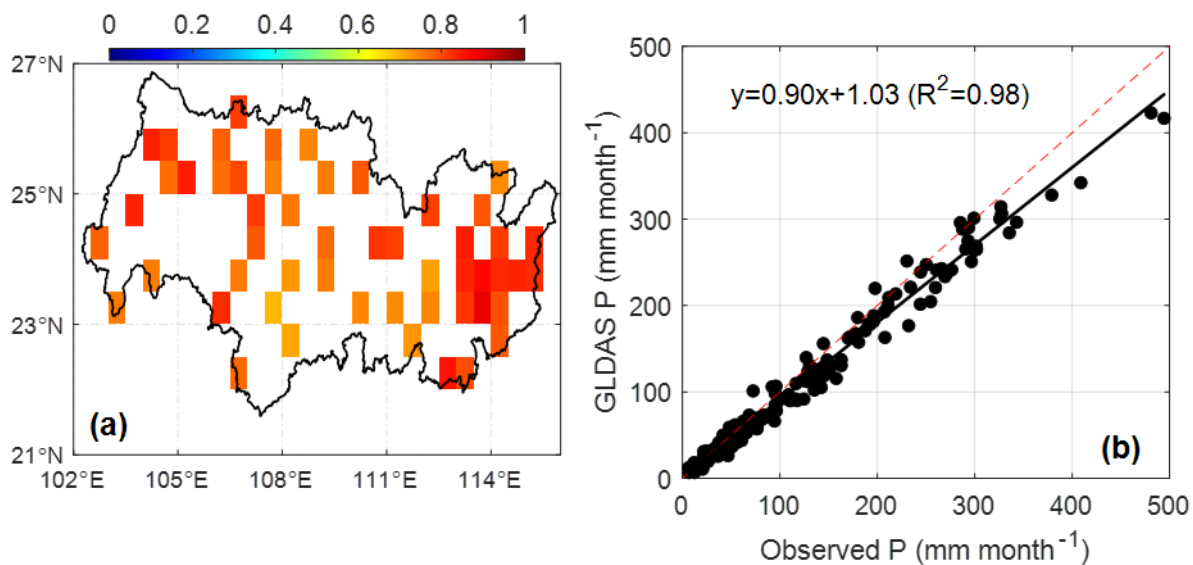


Figure 11. (a) Spatial distribution of R^2 between precipitation (P) from GLDAS and observations, and (b) scatter plot of monthly mean P over all pixels with stations available.

585